

1 **Individual and temporal variation in pathogen load predicts long-**
2 **term impacts of an emerging infectious disease**

3 Konstans Wells^{*1}, Rodrigo K. Hamede², Menna E. Jones², Paul A. Hohenlohe³, Andrew
4 Storfer⁴, Hamish I. McCallum¹

5

6 *1 Environmental Futures Research Institute, Griffith University, Brisbane QLD 4111,*
7 *Australia.*

8 *2 School of Biological Sciences, University of Tasmania, Private Bag 55, Hobart, Tasmania*
9 *7001, Australia.*

10 *3 Institute for Bioinformatics and Evolutionary Studies, Department of Biological Sciences,*
11 *University of Idaho, Moscow, ID 83844, USA.*

12 *4 School of Biological Sciences, Washington State University, Pullman, WA 99164-4236*
13 *USA.*

14

15 E-mail addresses (following order of authorship): konswells@gmail.com,

16 Rodrigo.HamedeRoss@utas.edu.au, MennaJones@utas.edu.au, hohenlohe@uidaho.edu,

17 astorfer@wsu.edu, h.mccallum@griffith.edu.au

18

19 *Corresponding author email: konswells@gmail.com

20

21 **Running head: Tasmanian devil facial tumour disease**

22

23

24

25

26 **Abstract**

27 Emerging infectious diseases increasingly threaten wildlife populations. Most studies focus
28 on managing short-term epidemic properties, such as controlling early outbreaks. Predicting
29 long-term endemic characteristics with limited retrospective data is more challenging. We
30 used individual-based modelling informed by individual variation in pathogen load and
31 transmissibility to predict long-term impacts of a lethal, transmissible cancer on Tasmanian
32 devil (*Sarcophilus harrisii*) populations. For this, we employed Approximate Bayesian
33 Computation to identify model scenarios that best matched known epidemiological and
34 demographic system properties derived from ten years of data after disease emergence,
35 enabling us to forecast future system dynamics. We show that the dramatic devil population
36 declines observed thus far are likely attributable to transient dynamics. Only 21% of
37 matching scenarios led to devil extinction within 100 years following devil facial tumour
38 disease (DFTD) introduction, whereas DFTD faded out in 57% of simulations. In the
39 remaining 22% of simulations, disease and host coexisted for at least 100 years, usually with
40 long-period oscillations. Our findings show that pathogen extirpation or host-pathogen
41 coexistence are much more likely than the DFTD-induced devil extinction, with crucial
42 management ramifications. Accounting for individual-level disease progression and the long-
43 term outcome of devil-DFTD interactions at the population-level, our findings suggest that
44 immediate management interventions are unlikely to be necessary to ensure the persistence of
45 Tasmanian devil populations. This is because strong population declines of devils after
46 disease emergence do not necessarily translate into long-term population declines at
47 equilibria. Our modelling approach is widely applicable to other host-pathogen systems to
48 predict disease impact beyond transient dynamics.

49

50

51 **Keywords**

52 disease burden; long-periodicity oscillation; population viability; Tasmanian devil;
53 transmissible cancer; wildlife health

54

55 **Introduction**

56 Emerging infectious diseases most often attract attention because their initial impacts on host
57 populations are frequently severe (de Castro and Bolker 2005, Smith et al. 2009). Following
58 the initial epidemic and transient dynamic behaviour, long-term outcomes include pathogen
59 fadeout, host extinction, or long-term endemicity with varying impacts on the host population
60 size (Hastings 2004, Benton et al. 2006, Cazelles and Hales 2006). Predicting which of these
61 long-term outcomes may occur on the basis of initial transient dynamics is very challenging
62 and conclusions about possible disease effects on population viability based on early
63 epidemic dynamics can be misleading.

64 Nevertheless, predicting the long-term consequences of an infectious disease as early
65 as possible in the emergence process is important for management. If the disease has a high
66 likelihood of ultimately leading to host extinction, then strategies such as stamping out
67 infection by removing all potentially infectious individuals may be justifiable, despite short-
68 term impacts on the host species and ethical considerations (McCallum and Hocking 2005).
69 Resource-intensive strategies such as establishing captive breeding populations protected
70 from disease or translocating individuals to locations separated from infected populations
71 may also be justified (McCallum and Jones 2006). In contrast, if impacts are transitory, then a
72 preferred strategy may be to avoid interference to allow a new long-term endemic disease
73 state or pathogen extinction to be reached as quickly as possible (Gandon et al. 2013).
74 Longer-term evolutionary processes can operate to ultimately reduce the impact of the

75 disease on the host population (Fenner 1983, Kerr 2012), and inappropriate disease
76 management strategies may slow down evolution of both host and pathogen.

77 Models of infectious diseases in the early stages of emergence typically focus on
78 estimating R_0 , the number of secondarily infected individuals when one infected individual is
79 introduced into a wholly susceptible population (Lloyd-Smith et al. 2005). This is a key
80 parameter for devising strategies to limit invasion or control an outbreak because it allows the
81 estimation of vaccination or removal rates necessary to eradicate disease. However, by
82 definition, it does not include density dependent factors and is therefore sometimes
83 insufficient to predict the long-term consequences of disease introduction into a new
84 population.

85 Most existing models for infectious disease are based around compartmental
86 Susceptible – Exposed – Infected – Recovered epidemiological models (S-E-I-R), which rely
87 on a strict assumption of homogeneity of individuals within compartments (Anderson and
88 May 1991). There is a parallel literature for macroparasitic infections, which assumes both a
89 stationary distribution of parasites amongst hosts and that parasite burden is determined by
90 the number of infective stages the host has encountered (Anderson and May 1978). For many
91 pathogens, pathogen load on (or inside) an individual typically changes following infection as
92 a result of within-host processes, causing temporal shifts in transmission and host mortality
93 rates. For example, the volume of transmissible tumours on Tasmanian devils (*Sarcophilus*
94 *harrisii*) increases through time, with measurable impacts on survival (Wells et al. 2017) and
95 likely temporal increases in transmission probability to uninfected devils that bite into the
96 growing tumour mass (Hamede et al. 2013). Similarly, increasing burden of the amphibian
97 chytrid fungus *Batrachochytrium dendrobatidis* on individual frogs after infection limits host
98 survival, with important consequences for disease spread and population dynamics (Briggs et
99 al. 2010, Wilber et al. 2016). Burdens of the causative agent of white nose syndrome,

100 *Pseudogymnoascus destructans*, which threatens numerous bat species in North America,
101 similarly increase on most individuals during the period of hibernation (Langwig et al. 2015).
102 The additional time dependence introduced by within-host pathogen growth can have a major
103 influence on the dynamics of host-pathogen interactions as uncovered by nested models that
104 link within- and between-host processes of disease dynamics (Gilchrist and Coombs 2006,
105 Mideo et al. 2008). Such dynamics are poorly captured by conventional compartmental and
106 macroparasite model structures. Thus, connecting across the scales of within- and between-
107 host dynamics remains a key challenge in understanding infectious disease epidemiology
108 (Gog et al. 2015).

109 Here we develop an individual-based model to explore the long-term impact of devil
110 facial tumour disease (DFTD), a transmissible cancer, on Tasmanian devil populations.
111 DFTD is a recently emerged infectious disease, first detected in 1996 in north-eastern
112 Tasmania (Hawkins et al. 2006). It is caused by a clonal cancerous cell line, which is
113 transmitted by direct transfer of live tumour cells when devils bite each other (Pearse and
114 Swift 2006, Jones et al. 2008, Hamede et al. 2013). DFTD is nearly always fatal and largely
115 affects individuals that are otherwise the fittest in the population (Wells et al. 2017).
116 Population declines to very low numbers concomitant with the frequency-dependent
117 transmission of DFTD led to predictions of devil extinctions, based on compartmental
118 epidemiological models (McCallum et al. 2009, Hamede et al. 2012).

119 Fortunately, the local devil extinctions predicted from these early models have not
120 occurred (McCallum et al. 2009). There is increasing evidence that rapid evolutionary
121 changes have taken place in infected devil populations, particularly in loci associated with
122 disease resistance and immune response (Epstein et al. 2016, Pye et al. 2016, Wright et al.
123 2017). Moreover, we recently reported that the force of infection (the rate at which
124 susceptible individuals become infected) increases over a time period of as long as six years

125 (~3 generations) after initial local disease emergence and that the time until death after initial
126 infection may be as long as two years (Wells et al. 2017). Therefore, despite high lethality,
127 the rate of epidemic increase appears to be relatively slow, prompting predictive modelling of
128 population level impacts over time spans well beyond those covered by field observations.

129 In general, there are three potential long-term outcomes of host-pathogen interactions:
130 host extinction, pathogen extirpation, and host-pathogen coexistence. To determine the
131 likelihood of each of these outcomes in a local population of Tasmanian devils, we used
132 individual-based simulation modelling (**Figure 1**) and pattern matching, based on ten years of
133 existing field data, to project population trajectories for Tasmanian devil populations over
134 100 years following DFTD introduction.

135

136 **Materials and methods**

137 *Model framework*

138 We implemented a stochastic individual-based simulation model of coupled Tasmanian devil
139 (*Sarcophilus harrisi*) demography and devil facial tumour disease (DFDT) epidemiology. A
140 full model description with overview of design, concept, and details (Grimm et al. 2006) can
141 be found in SI Appendix 1. In brief, we aimed to simulate the impact of DFTD on Tasmanian
142 devil populations and validate 10^6 model scenarios of different random input parameters (26
143 model parameters assumed to be unknown and difficult or impossible to estimate from
144 empirical studies, see Supporting Information **Table S1**) by matching known system level
145 properties (disease prevalence and population structure) derived from a wild population
146 studied over ten years after the emergence of DFTD (Hamede et al. 2015). In particular,
147 running model scenarios for 100 years prior to, and after the introduction of DFTD, we
148 explored the extent to which DFTD causes devil populations to decline or become extinct.
149 Moreover, we aimed to explore whether input parameters such as the latency period of DFTD

150 or the frequencies of disease transmission between individuals of different ages can be
151 identified by matching simulation scenarios to field patterns of devil demography and disease
152 prevalence.

153 Entities in the model are individuals that move in weekly time steps (movement
154 distance θ) within their home ranges and may potentially engage in disease-transmitting
155 biting behaviour with other individuals (**Fig 1**). Birth-death processes and DFTD
156 epidemiology are modelled as probabilities according to specified input parameter values for
157 each scenario. In each time step, processes are scheduled in the following order: 1)
158 reproduction of mature individuals (if the week matches the reproductive season), 2)
159 recruitment of juveniles into the population, 3) natural death (independent of DFTD), 4)
160 physical interaction and potential disease transmission, 5) growth of tumours, 6) DFTD-
161 induced death, 7) movement of individuals, 8) aging of individuals.

162 The force of infection $\lambda_{i,t}$, i.e. the probability that a susceptible individual i acquires
163 DFTD at time t is given as the sum of the probabilities of DFTD being transmitted from any
164 interacting infected individual k (with $k \in 1 \dots K$, with K being the number of all individuals in
165 the population excluding i):

$$166 \quad \lambda_i = \left[\sum_{k \in K} \beta_{A(i)} \beta_{A(k)} \left(\frac{N_t}{C} \right)^\delta \left(\frac{1}{1+(1-r_{i,t})\omega} \right) \left(\frac{1}{1+(1-r_{k,t})\omega} \right) \left(\frac{V_{k,t}}{V_{max}} \right)^\gamma \right] I_\eta$$

167 Here, the disease transmission coefficient is composed of the two factors $\beta_{A(i)}$ and $\beta_{A(k)}$, each
168 of which accounts for the age-specific interaction and disease transmission rate for
169 individuals i and k according to their age classes A . N_t is the population size at time t ; the
170 scaling factor δ accounts for possible increase in interactions frequency with increasing
171 population size if $\delta > 0$. The parameter $r_{i,t}$ is a Boolean indicator of whether an individual
172 recently reproduced and ω is a scaling factor that determines the difference in $\lambda_{i,t}$ resulting
173 from interactions of reproductively active and non-reproducing individuals. $V_{k,t}$ is the tumour

174 load of individual k , V_{max} is the maximum tumour load, and γ is a scaling factor of how $\lambda_{i,t}$
175 changes with tumour load of infected individuals. The parameter I_η is a Boolean indicator of
176 whether two individuals are located in a spatial distance $< \eta$ that allows interaction and
177 disease transmission (i.e. only individuals in distances $< \eta$ can infect each other). We
178 considered individuals as ‘reproductively active’ ($r_{i,t}=1$) for eight weeks after a reproduction
179 event.

180 DFTD-induced mortality Ω_{size} accounts for tumour size, while tumour growth was
181 modelled as a logistic function with the growth parameter α sampled as an input parameter.
182 We allowed for latency periods τ between infection and the onset of tumour growth, which
183 was also sampled as an input parameter. We assumed no recovery from DFTD, which
184 appears to be very rare in the field (Pye et al. 2016).

185 Notably, sampled scaling factor values of zero for δ , ω , and γ correspond to model
186 scenarios with homogeneous interaction frequencies and disease transmission rates
187 independent of population size, reproductive status and tumour load, respectively, while
188 values of $\eta = 21$ km assume that individuals can infect each other independent of spatial
189 proximity (i.e. individuals across the entire study area can infect each other). The sampled
190 parameter space included scenarios that omitted *i*) effects of tumour load on infection and
191 survival propensity, *ii*) effect of spatial proximity on the force of infection between pairs of
192 individuals and *iii*) both effects of tumour load and spatial proximity, in each of 1,000
193 scenarios. This sampling design was used to explicitly assess the importance of modelling
194 individual tumour load and space use for accurately representing the system dynamics.

195

196 ***Model validation and summary***

197 To resolve the most realistic model structures and assumptions from a wide range of
198 possibilities and to compare simulation output with summary statistics from our case study (a

199 devil population at West Pencil Pine in western Tasmania) (Wells et al. 2017), we used
200 likelihood-free Approximate Bayesian Computation (ABC) for approximating the most likely
201 input parameter values, based on the distances between observed and simulated summary
202 statistics (Toni et al. 2009). We used the ‘neuralnet’ regression method in the R package *abc*
203 (Csillery et al. 2012). Prediction error was minimized by determining the most accurate
204 tolerance rate and corresponding number of scenarios considered as posterior through a
205 subsampling cross validation procedure as implemented in the *abc* package. For this, leave-
206 one-out cross validation was used to evaluate the out-of-sample accuracy of parameter
207 estimates (using a subset of 100 randomly selected simulated scenarios), with a prediction
208 error estimated for each input parameter (Csillery et al. 2012); this step facilitates selecting
209 the most accurate number of scenarios as a posterior sample. However, we are aware that
210 none of the scenarios selected as posterior samples entirely represents the true system
211 dynamics. We identified $n = 122$ scenarios (tolerance rate of 0.009, Supporting Information
212 **Figure S1**) as a reasonable posterior selection with minimized prediction error but
213 sufficiently large sample size to express uncertainty in estimates. The distribution of
214 summary statistics was tested against the summary statistics from our case study as a
215 goodness of fit test, using the ‘gfit’ function in the *abc* package (with a p-value of 0.37
216 indicating reasonable fit, see Supporting Information **Figure S2, S3**).

217 We generated key summary statistics from the case study, in which DFTD was
218 expected to have been introduced shortly before the onset of the study (Hamede et al. 2015),
219 and a pre-selection of simulation scenarios, in which juveniles never comprised > 50% of the
220 population, DFTD prevalence at end of 10-year-period was between 10 and 70%, and the age
221 of individuals with growing tumours was ≥ 52 weeks. Hereafter, we refer to ‘prevalence’ as
222 the proportion of free-ranging devil individuals (animals ≥ 35 weeks old) with tumours of
223 sizes $\geq 0.1 \text{ cm}^3$; we do so to derive a measure of prevalence from simulations that is

224 comparable to those inferred from field data. Summary statistics were: 1) mean DFTD
225 prevalence over the course of 10 years, 2) mean DFTD prevalence in the 10th year only, 3)
226 autocorrelation value for prevalence values lagged over one time step, 4) three coefficient
227 estimates of a cubic regression model of the smoothed ordered difference in DFTD
228 prevalence (fitting 3rd order orthogonal polynomials of time for smoothed prevalence values
229 using the loess function in R with degree of smoothing set to $\alpha = 0.75$), 5) phase in seasonal
230 population fluctuations, calculated from sinusoidal model fitted to the number of trappable
231 individuals in different time steps, 6) regression coefficient of a linear model of the changing
232 proportions of individuals ≥ 3 years old in the trappable population over the course of ten
233 years. Summary statistics for the simulations were based on the 37 selected weekly time steps
234 after the introduction of DFTD that matched the time sequences of capture sessions in the
235 case study, which included records in ca. three months intervals (using the first 30 time steps
236 only for population sizes, as the empirical estimates from the last year of field data may be
237 subject to data censoring bias). Overall, these summary statistics aimed to describe general
238 patterns rather than reproducing the exact course of population and disease prevalence
239 changes over time, given that real systems would not repeat themselves for any given
240 dynamics (Wood 2010). Additionally, unknown factors not considered in the model may
241 contribute to the observed temporal changes in devil abundance and disease prevalence.

242 As results from our simulations, we considered the posterior distributions of the
243 selected input parameters (as adjusted parameter values according to the ABC approach
244 utilised) and calculated the frequency and timing of population or disease extirpation from
245 the 100 years of simulation after DFTD introduction of the selected scenarios. All simulations
246 and statistics were performed in R version 3.4.3 (R Development Core Team 2017). We used
247 wavelet analysis based on Morlet power spectra as implemented in the R package
248 *WaveletComp* (Roesch and Schmidbauer 2014) to identify possible periodicity at different

249 frequencies in the time series of population sizes (based on all free-ranging individuals) for
250 scenarios in which DFTD persisted at least 100 years.

251

252 **Results**

253 For scenarios that best matched empirical mark-recapture data, 21% of scenarios (26 out of
254 122) led to devil population extirpation in timespans of 13 – 42 years (mean = 21, SD = 8;
255 ~7-21 generations) after introduction of DFTD (**Figure 2**). In contrast, the disease was lost in
256 57% of these scenarios (69 out of 122), with disease extirpation taking place 11 – 100 years
257 (mean = 29, SD = 22) post-introduction (**Figure 2**). Loss of DFTD from local populations
258 therefore appears to be much more likely than devil population extirpation, given no other
259 factor than DFTD reducing devil vital rates. Moreover, fluctuations in host and pathogen
260 after the introduction of DFTD exhibited long-period oscillations in most cases (**Figure 3**). In
261 the 27 selected scenarios in which DFTD persisted in populations for 100 years after disease
262 introduction, population size 80-100 years after disease introduction was smaller and more
263 variable (mean = 137, SD = 36) than population sizes prior to the introduction of DFTD
264 (mean = 285, SD = 3; **Figure 4**). The average DFTD prevalence 80-100 years after disease
265 introduction remained < 40% (mean = 14%, SD = 4%; **Figure 4**). Most wavelet power
266 spectra of these scenarios showed long-period oscillations over time periods between 261 –
267 1040 weeks (corresponding to 5 – 20 years) (electronic supplementary material, Supporting
268 Information **Figure S4**).

269 Inference of input parameters was only possible for some parameters, whereas 95%
270 credible intervals for most of the posterior distributions were not distinguishable from the
271 (uniformly) sampled priors. Notably, the posterior mode for the latency period (τ) was
272 estimated as 50.5 weeks (95% credible interval 48.5 – 52.6 weeks, for unadjusted parameters
273 values the 95% was 22.9 – 94.3 weeks), providing a first estimate of this latent parameter

274 from field data (Supporting Information **Figure S5, Table S2**). The posterior of the DFTD-
275 induced mortality factor (odds relative to un-diseased devils) for tumours $< 50 \text{ cm}^3$ ($\Omega_{<50}$)
276 was constrained to relatively large values (electronic supplementary material, Supporting
277 Information **Figure S5**), supporting empirical estimates that small tumours are unlikely to
278 cause significant mortality of devils. Posterior distributions of weekly movement distances
279 (θ) and the spatial distance over which disease-transmitting interactions took place (η), in
280 turn, allowed no clear estimates of these parameters (electronic supplementary material,
281 Supporting Information **Figure S5**). Notably, the 122 scenarios selected as posteriors all
282 explicitly accounted for the effect of tumour load on infection and survival, while 90% of
283 selected scenarios included spatial proximity of individuals as influencing disease
284 transmission (i.e. selected scenarios comprised 110 models that included both the effect of
285 tumour load and spatial proximity, while 12 models included tumour load but not spatial
286 proximity).

287

288 **Discussion**

289 Our results suggest that DFTD will not necessarily cause local Tasmanian devil extinction or
290 even long-term major declines, whereas the extirpation of DFTD or coexistence/endemicity is
291 much more likely. In cases where DFTD persists in local devil populations in the long-term,
292 oscillations with relatively long periods (5-20 years, corresponding to 2-10 generations)
293 appear likely. These predictions are starkly different from those derived from previous
294 compartmental models, which considered all devils with detectable tumours to be equally
295 infectious and assumed exponentially distributed time delays. These models predicted
296 extinction (McCallum et al. 2009), as did models with more realistic gamma distributed time
297 delays or with delay-differential equations that incorporated field-derived parameter
298 estimates of transmission and mortality rates (Beeton and McCallum 2011). These previous

299 models, however, differ also from our approach in that they ignore spatial structure and do
300 not account for the uncertainty in unknown parameters such as disease-induced mortality and
301 disease transmission rates.

302 The predictions from our individually-based model, derived from 10 years of
303 observational data at our case study site (West Pencil Pine), are consistent with observations
304 now emerging from long-term field studies of the dynamics of Tasmanian devils and DFTD
305 (Lazenby et al. 2018). No Tasmanian devil population has yet become extinct – and
306 populations persist, albeit in low numbers, where disease has been present the longest (e.g., at
307 wukalina/Mount William National Park and at Freycinet, where DFTD emerged,
308 respectively, at least 21 and 17 years ago) (Epstein et al. 2016). Also, a considerable decline
309 in DFTD prevalence has been observed in recent years at Freycinet (Sebastien Comte,
310 unpublished data). These study sites did not contribute to the fitting of our model and at least
311 to some extent constitute an independent validation and test of the model predictions. Our
312 modelling results suggest that observed population dynamics of devils and DFTD do not
313 require evolutionary changes, although there is evidence of rapid evolution in disease-
314 burdened devil populations (Epstein et al. 2016) similar to rapid evolution in other vertebrates
315 when subjected to intense selection pressure (Christie et al. 2016, Campbell-Staton et al.
316 2017).

317 One of the differences between earlier models and those we present here is the
318 inclusion of tumour growth, with mortality and transmission rates that depend on individual
319 disease burden. Inclusion of burden-dependent dynamics results in additional and
320 qualitatively different time delays than those incorporated in previous models. Tumours take
321 time to grow before they have a major impact on host survival and become highly infectious
322 (Hamede et al. 2017, Wells et al. 2017). This slows the spread of DFTD and its impact on
323 devil population fluctuations. It also means that parameters estimated from field data, without

324 taking tumour growth into account, do not adequately represent the system dynamics
325 (McCallum et al. 2009). Our models suggest that documented dramatic population declines
326 during the first 10 years or so of the DFTD epizootic may represent just the first peak of a
327 classical epidemic (Bailey 1975). Long-term predictions from our models suggest, however,
328 that DFTD is a slow burning disease with population changes governed by long-term
329 oscillations.

330 It is well known, both from simple Lotka-Volterra models and from a range of
331 empirical studies, that consumer–resource interactions have a propensity to cycle, driven by
332 the time delays inherent in these systems (Murdoch et al. 2003). Disease burden-dependent
333 demographic and epidemiological parameters, together with burden growth within the host,
334 add additional time delays, both lengthening any oscillations and increasing the likelihood
335 that they will be maintained in the longer term. Apparently, such time-delays increase the
336 probability of host-pathogen coexistence, similar to predator-prey dynamics, rather than host
337 or pathogen extirpation. Grounded in theory and a reasonable body of modelling studies of
338 other wildlife diseases, disease-induced population extinction appears to be more generally an
339 exception rather than the rule, unless host populations are very small, or unless there are
340 reservoir species that are tolerant of infection (de Castro and Bolker 2005).

341

342 The approach we apply here – coupling the flexibility of individual-based models to account
343 for heterogeneity in disease burden and space use with Approximate Bayesian Computation
344 to match model outcomes with available empirical evidence - offers considerable potential
345 for making predictions regarding the population dynamics for other emerging diseases (Toni
346 et al. 2009, Beaumont 2010, Johnson and Briggs 2011, Wells et al. 2015). A fundamental
347 problem in applying modelling approaches to forecast the outcome of emerging infectious
348 disease epidemics is the need to estimate parameter values based on empirical data derived

349 from the relatively early stages of an epizootic, in the absence of retrospective knowledge
350 (Heesterbeek et al. 2015, Ferguson et al. 2016). Examples include estimating R_0 for SARS
351 (Lipsitch et al. 2003) and for the 2014-2015 Ebola epidemic in West Africa (Whitty et al.
352 2014, WHO Ebola Response Team 2014) among others (LaDeau et al. 2011). In most of
353 these cases, the objective is to estimate parameters associated with the growth phase of the
354 epidemic to assess the effectiveness of interventions such as vaccination. The task we have
355 addressed in this paper is even more challenging – seeking to predict the long-term endemic
356 behaviour of a pathogen that is currently still in the early stages of emergence. We suggest
357 that management efforts to maintain devil populations in the face of DFTD should be guided
358 by our changing understanding of the long-term dynamics of the DFTD epidemic.

359 Management efforts in wild populations that solely aim to combat the impact of DFTD can
360 be counterproductive if they disrupt long-term eco-evolutionary dynamics that may
361 eventually lead to endemicity with stable devil populations. Our ability to predict future
362 outcomes in the absence of management actions require some caution as we cannot fully
363 exclude the possibility that DFTD can cause local population extinctions once populations are
364 small, warranting future research. While our findings emphasize the importance of
365 accounting for individual tumour load for accurate prediction and epidemiological modelling
366 of DFTD dynamics, our inability to uncover the exact role of devil spatial proximity on
367 disease transmission means that further research is necessary to understand relevant factors in
368 disease spread.

369

370 The key management implication of our model is that "heroic" management interventions are
371 unlikely to be necessary to ensure persistence of Tasmanian devil populations. Given more
372 information on immune-related or genetic variation in resistance, the model could be
373 modified to assess the value of interventions such as vaccination or reintroduction of captive

374 reared animals. At the same time, we believe that any management actions should be subject
375 to rigorous quantitative analysis to explore possible long-term impacts. In particular,
376 allocating resources and scientific endeavours to the management of wildlife diseases such as
377 DFTD should not disguise the fact that sufficiently large and undisturbed natural
378 environments are a vital prerequisite for wildlife to persist and eventually cope with
379 perturbations such as infectious diseases without human intervention.

380

381

382 **Acknowledgments**

383 The study was funded by NSF grant DEB 1316549 and NIH grant R01 GM126563-01 as part
384 of the joint NIH-NSF-USDA Ecology and Evolution of Infectious Diseases Program, the
385 Australian Research Council Discovery (DP110102656), Future Fellowship (FT100100250),
386 DECRA (DE17010116) and Linkage (LP0561120, LP0989613) Schemes, the Fulbright
387 Scholarship Scheme, the Ian Potter Foundation, the Australian Academy of Science
388 (Margaret Middleton Fund), two grants from the Estate of W.V. Scott, the National
389 Geographic Society, the Mohammed bin Zayed Conservation Fund, the Holsworth Wildlife
390 Trust and three Eric Guiler Tasmanian Devil Research Grants through the Save the
391 Tasmanian Devil Appeal of the University of Tasmania Foundation. We are grateful for all
392 support during field work underpinning this modelling study: M. and C. Walsh, Discovery
393 Holidays Parks-Cradle Mountain National Park, and Forico Pty Ltd provided logistic support
394 and many volunteers helped with data collection (published previously). Comments from
395 Samuel Alizon and anonymous reviewers improved previous drafts.

396

397 **Authors' contribution**

398 K.W. conceived the idea of this study, carried out the analysis and wrote the first draft. All
399 authors interpreted results and contributed to revisions. All authors gave final approval for
400 publication.

401

402

403

404

405

406

407

408

409

410

411

412

413

414

415

416

417

418

419

420

421

422

423 **References**

- 424 Anderson, R. M., and R. M. May. 1978. Regulation and stability of host-parasite population
425 interactions: 1. regulatory processes. *Journal of Animal Ecology* 47:219-247.
- 426 Anderson, R. M., and R. M. May. 1991. *Infectious diseases of humans: dynamics and*
427 *control*. Oxford University Press, Oxford.
- 428 Bailey, N. T. J. 1975. *The mathematical theory of infectious diseases and its applications*. 2nd
429 edition. Charles Griffin.
- 430 Beaumont, M. A. 2010. Approximate Bayesian Computation in evolution and ecology.
431 *Annual Review of Ecology, Evolution, and Systematics* 41:379-406.
- 432 Beeton, N., and H. McCallum. 2011. Models predict that culling is not a feasible strategy to
433 prevent extinction of Tasmanian devils from facial tumour disease. *Journal of Applied*
434 *Ecology* 48:1315-1323.
- 435 Benton, T. G., S. J. Plaistow, and T. N. Coulson. 2006. Complex population dynamics and
436 complex causation: devils, details and demography. *Proceedings of the Royal Society*
437 *Biological Sciences Series B*. 273:1173-1181.
- 438 Briggs, C. J., R. A. Knapp, and V. T. Vredenburg. 2010. Enzootic and epizootic dynamics of
439 the chytrid fungal pathogen of amphibians. *Proceedings of the National Academy of*
440 *Sciences* 107:9695-9700.
- 441 Campbell-Staton, S. C., Z. A. Cheviron, N. Rochette, J. Catchen, J. B. Losos, and S. V.
442 Edwards. 2017. Winter storms drive rapid phenotypic, regulatory, and genomic shifts
443 in the green anole lizard. *Science* 357:495-498.
- 444 Cazelles, B., and S. Hales. 2006. Infectious diseases, climate influences, and nonstationarity.
445 *Plos Medicine* 3:e328.

- 446 Christie, M. R., M. L. Marine, S. E. Fox, R. A. French, and M. S. Blouin. 2016. A single
447 generation of domestication heritably alters the expression of hundreds of genes.
448 *Nature Communications* 7:10676.
- 449 Csillery, K., O. Francois, and M. G. B. Blum. 2012. abc: an R package for approximate
450 Bayesian computation (ABC). *Methods in Ecology and Evolution* 3:475-479.
- 451 de Castro, F., and B. Bolker. 2005. Mechanisms of disease-induced extinction. *Ecology*
452 *Letters* 8:117-126.
- 453 Epstein, B., M. Jones, R. Hamede, S. Hendricks, H. McCallum, E. P. Murchison, B.
454 Schönfeld, C. Wiench, P. Hohenlohe, and A. Storfer. 2016. Rapid evolutionary
455 response to a transmissible cancer in Tasmanian devils. *Nature Communications*
456 7:12684.
- 457 Fenner, F. 1983. Biological control as exemplified by smallpox eradication and myxomatosis.
458 *Proceedings of the Royal Society B: Biological Sciences* 218:259-285.
- 459 Ferguson, N. M., Z. M. Cucunubá, I. Dorigatti, G. L. Nedjati-Gilani, C. A. Donnelly, M.-G.
460 Basáñez, P. Nouvellet, and J. Lessler. 2016. Countering the Zika epidemic in Latin
461 America. *Science* 353:353-354.
- 462 Gandon, S., M. E. Hochberg, R. D. Holt, and T. Day. 2013. What limits the evolutionary
463 emergence of pathogens? *Philosophical Transactions of the Royal Society B:*
464 *Biological Sciences* 368.
- 465 Gilchrist, M. A., and D. Coombs. 2006. Evolution of virulence: interdependence, constraints,
466 and selection using nested models. *Theoretical Population Biology* 69:145-153.
- 467 Gog, J. R., L. Pellis, J. L. N. Wood, A. R. McLean, N. Arinaminpathy, and J. O. Lloyd-
468 Smith. 2015. Seven challenges in modeling pathogen dynamics within-host and across
469 scales. *Epidemics* 10:45-48.

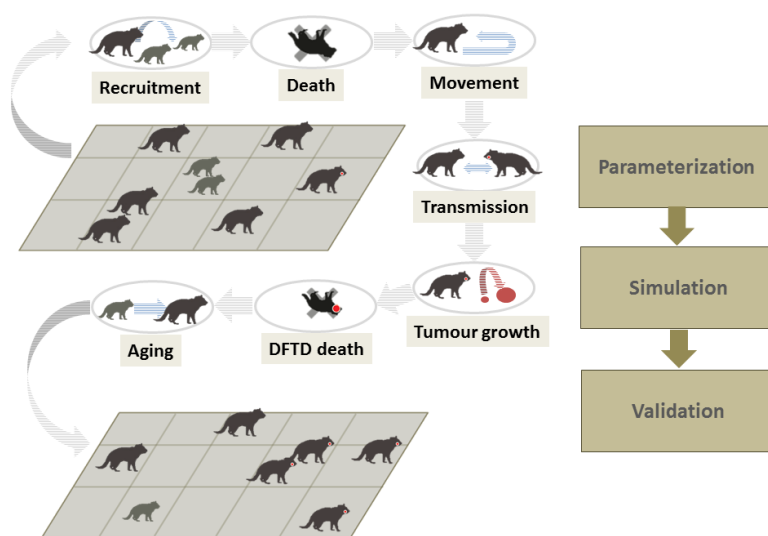
- 470 Grimm, V., U. Berger, F. Bastiansen, S. Eliassen, V. Ginot, J. Giske, J. Goss-Custard, T.
471 Grand, S. K. Heinz, G. Huse, A. Huth, J. U. Jepsen, C. Jorgensen, W. M. Mooij, B.
472 Mueller, G. Pe'er, C. Piou, S. F. Railsback, A. M. Robbins, M. M. Robbins, E.
473 Rossmannith, N. Rueger, E. Strand, S. Souissi, R. A. Stillman, R. Vabo, U. Visser, and
474 D. L. DeAngelis. 2006. A standard protocol for describing individual-based and
475 agent-based models. *Ecological Modelling* 198:115-126.
- 476 Hamede, R., J. Bashford, M. Jones, and H. McCallum. 2012. Simulating devil facial tumour
477 disease outbreaks across empirically derived contact networks. *Journal of Applied
478 Ecology* 49:447-456.
- 479 Hamede, R. K., N. J. Beeton, S. Carver, and M. E. Jones. 2017. Untangling the model
480 muddle: empirical tumour growth in Tasmanian devil facial tumour disease. *Scientific
481 Reports* 7:6217.
- 482 Hamede, R. K., H. McCallum, and M. Jones. 2013. Biting injuries and transmission of
483 Tasmanian devil facial tumour disease. *Journal of Animal Ecology* 82:182-190.
- 484 Hamede, R. K., A.-M. Pearse, K. Swift, L. A. Barmuta, E. P. Murchison, and M. E. Jones.
485 2015. Transmissible cancer in Tasmanian devils: localized lineage replacement and
486 host population response. *Proceedings of the Royal Society of London B: Biological
487 Sciences* 282:20151468.
- 488 Hastings, A. 2004. Transients: the key to long-term ecological understanding? *Trends in
489 Ecology & Evolution* 19:39-45.
- 490 Hawkins, C. E., C. Baars, H. Hesterman, G. J. Hocking, M. E. Jones, B. Lazenby, D. Mann,
491 N. Mooney, D. Pemberton, S. Pyecroft, M. Restani, and J. Wiersma. 2006. Emerging
492 disease and population decline of an island endemic, the Tasmanian devil *Sarcophilus
493 harrisii*. *Biological Conservation* 131:307-324.

- 494 Heesterbeek, H., R. M. Anderson, V. Andreasen, S. Bansal, D. De Angelis, C. Dye, K. T. D.
495 Eames, W. J. Edmunds, S. D. W. Frost, S. Funk, T. D. Hollingsworth, T. House, V.
496 Isham, P. Klepac, J. Lessler, J. O. Lloyd-Smith, C. J. E. Metcalf, D. Mollison, L.
497 Pellis, J. R. C. Pulliam, M. G. Roberts, C. Viboud, and I. N. I. I. Collaboration. 2015.
498 Modeling infectious disease dynamics in the complex landscape of global health.
499 Science 347.
- 500 Johnson, L. R., and C. J. Briggs. 2011. Parameter inference for an individual based model of
501 chytridiomycosis in frogs. *Journal of Theoretical Biology* 277:90-98.
- 502 Jones, M. E., A. Cockburn, R. Hamede, C. Hawkins, H. Hesterman, S. Lachish, D. Mann, H.
503 McCallum, and D. Pemberton. 2008. Life-history change in disease-ravaged
504 Tasmanian devil populations. *Proceedings of the National Academy of Sciences of*
505 *the United States of America* 105:10023-10027.
- 506 Kerr, P. J. 2012. Myxomatosis in Australia and Europe: a model for emerging infectious
507 diseases. *Antiviral Research* 93:387-415.
- 508 LaDeau, S. L., G. E. Glass, N. T. Hobbs, A. Latimer, and R. S. Ostfeld. 2011. Data-model
509 fusion to better understand emerging pathogens and improve infectious disease
510 forecasting. *Ecological Applications* 21:1443-1460.
- 511 Langwig, K. E., W. F. Frick, R. Reynolds, K. L. Parise, K. P. Drees, J. R. Hoyt, T. L. Cheng,
512 T. H. Kunz, J. T. Foster, and A. M. Kilpatrick. 2015. Host and pathogen ecology drive
513 the seasonal dynamics of a fungal disease, white-nose syndrome. *Proceedings of the*
514 *Royal Society B-Biological Sciences* 282.
- 515 Lazenby, B. T., M. W. Tobler, W. E. Brown, C. E. Hawkins, G. J. Hocking, F. Hume, S.
516 Huxtable, P. Iles, M. E. Jones, C. Lawrence, S. Thalmann, P. Wise, H. Williams, S.
517 Fox, and D. Pemberton. 2018. Density trends and demographic signals uncover the

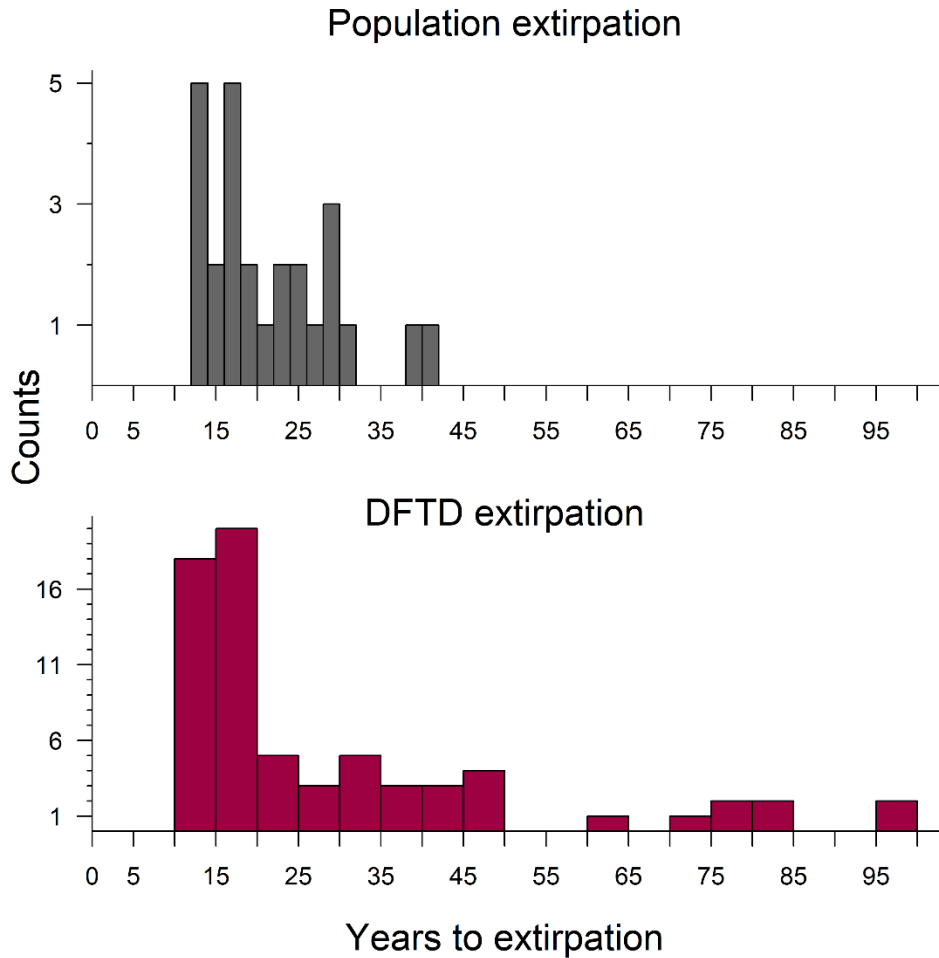
- 518 long-term impact of transmissible cancer in Tasmanian devils. *Journal of Applied*
519 *Ecology*:n/a-n/a.
- 520 Lipsitch, M., T. Cohen, B. Cooper, J. M. Robins, S. Ma, L. James, G. Gopalakrishna, S. K.
521 Chew, C. C. Tan, M. H. Samore, D. Fisman, and M. Murray. 2003. Transmission
522 dynamics and control of severe acute respiratory syndrome. *Science* 300:1966-1970.
- 523 Lloyd-Smith, J. O., P. C. Cross, C. J. Briggs, M. Daugherty, W. M. Getz, J. Latta, M. S.
524 Sanchez, A. B. Smith, and A. Sweil. 2005. Should we expect population thresholds for
525 wildlife disease? *Trends in Ecology & Evolution* 20:511-519.
- 526 McCallum, H., and B. A. Hocking. 2005. Reflecting on ethical and legal issues in wildlife
527 disease. *Bioethics* 19:336-347.
- 528 McCallum, H., and M. Jones. 2006. To lose both would look like carelessness: Tasmanian
529 devil facial tumour disease. *Plos Biology* 4:1671-1674.
- 530 McCallum, H., M. Jones, C. Hawkins, R. Hamede, S. Lachish, D. L. Sinn, N. Beeton, and B.
531 Lazenby. 2009. Transmission dynamics of Tasmanian devil facial tumor disease may
532 lead to disease-induced extinction. *Ecology* 90:3379-3392.
- 533 Mideo, N., S. Alizon, and T. Day. 2008. Linking within- and between-host dynamics in the
534 evolutionary epidemiology of infectious diseases. *Trends in Ecology & Evolution*
535 23:511-517.
- 536 Murdoch, W. W., C. J. Briggs, and R. M. Nisbet. 2003. *Consumer-resource dynamics*.
537 Princeton University Press.
- 538 Pearse, A. M., and K. Swift. 2006. Allograft theory: transmission of devil facial-tumour
539 disease. *Nature* 439:549-549.
- 540 Pye, R., R. Hamede, H. V. Siddle, A. Caldwell, G. W. Knowles, K. Swift, A. Kreiss, M. E.
541 Jones, A. B. Lyons, and G. M. Woods. 2016. Demonstration of immune responses
542 against devil facial tumour disease in wild Tasmanian devils. *Biology letters* 12.

- 543 R Development Core Team. 2017. R: A language and environment for statistical computing.
544 R Foundation for Statistical Computing, Vienna, Austria.
- 545 Roesch, A., and H. Schmidbauer. 2014. WaveletComp: computational wavelet analysis. R
546 package version 1.0.
- 547 Smith, K. F., K. Acevedo-Whitehouse, and A. B. Pedersen. 2009. The role of infectious
548 diseases in biological conservation. *Animal Conservation* 12:1-12.
- 549 Toni, T., D. Welch, N. Strelkowa, A. Ipsen, and M. P. H. Stumpf. 2009. Approximate
550 Bayesian computation scheme for parameter inference and model selection in
551 dynamical systems. *Journal of the Royal Society Interface* 6:187-202.
- 552 Wells, K., B. W. Brook, R. C. Lacy, G. J. Mutze, D. E. Peacock, R. G. Sinclair, N.
553 Schwensow, P. Cassey, R. B. O'Hara, and D. A. Fordham. 2015. Timing and severity
554 of immunizing diseases in rabbits is controlled by seasonal matching of host and
555 pathogen dynamics. *Journal of the Royal Society Interface* 12:20141184.
- 556 Wells, K., R. Hamede, D. H. Kerlin, A. Storfer, P. A. Hohenlohe, M. E. Jones, and H. I.
557 McCallum. 2017. Infection of the fittest: devil facial tumour disease has greatest
558 effect on individuals with highest reproductive output. *Ecology Letters* 20:770-778.
- 559 Whitty, C. J. M., J. Farrar, N. Ferguson, W. J. Edmunds, P. Piot, M. Leach, and S. C. Davies.
560 2014. Tough choices to reduce Ebola transmission. *Nature* 515:192-194.
- 561 WHO Ebola Response Team. 2014. Ebola virus disease in West Africa - the first 9 months of
562 the epidemic and forward projections. *New England Journal of Medicine* 371:1481-
563 1495.
- 564 Wilber, M. Q., K. E. Langwig, A. M. Kilpatrick, H. I. McCallum, and C. J. Briggs. 2016.
565 Integral projection models for host-parasite systems with an application to amphibian
566 chytrid fungus. *Methods in Ecology and Evolution* 10:1182-1194

567 Wood, S. N. 2010. Statistical inference for noisy nonlinear ecological dynamic systems.
568 Nature 466:1102–1104.
569 Wright, B., C. E. Willet, R. Hamede, M. Jones, K. Belov, and C. M. Wade. 2017. Variants in
570 the host genome may inhibit tumour growth in devil facial tumours: evidence from
571 genome-wide association. Scientific Reports 7:423.
572



573
574 **Figure 1.** Illustrative overview of the individual-based model to explore long-term population
575 changes of a Tasmanian devil population burdened with devil facial tumour disease (DFTD).
576 Individuals are distributed in a study area. For every weekly time step seven different
577 processes are modelled, namely 1) the possible recruitment of young from females
578 (conditional on young survival during previous weaning time), 2) possible death independent
579 of disease status, 3) movement of individuals away from their home range centre, 4)
580 behavioural interaction between nearby individuals that may result in the transmission of
581 DFTD, 5) growth of DFTD tumours, 6) death of individuals resulting from DFTD, 7) aging
582 of individuals.
583



584

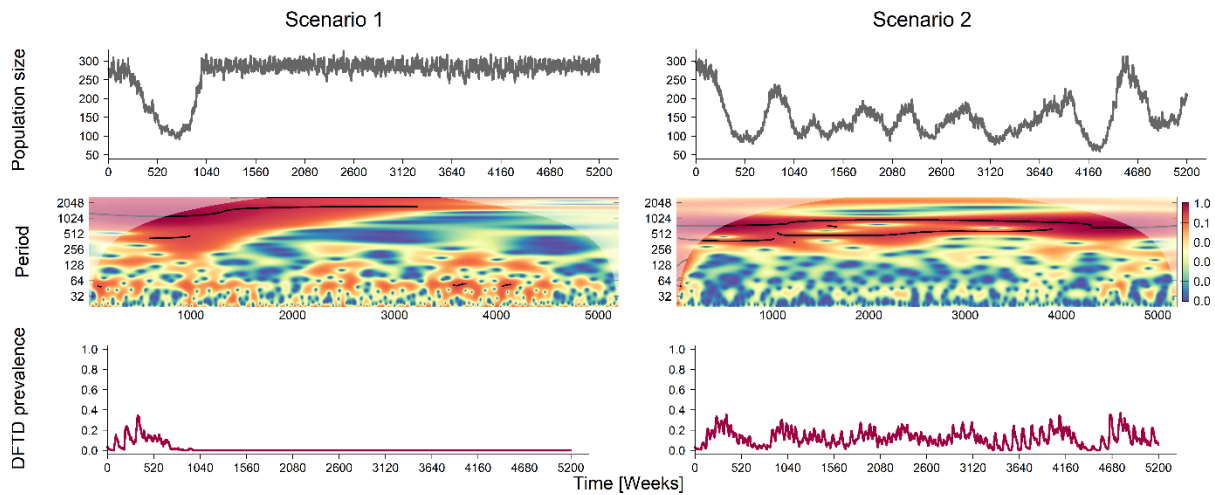
585 **Figure 2.** Frequency distributions of timespans of devil extirpation (upper panel) and devil
586 facial tumour disease (DFTD) extirpation presented as years after the introduction of the
587 disease into populations. Number of plotted scenarios correspond to those for which
588 extirpation events were recorded (26 and 69 out of 122 posterior samples, respectively).

589

590

591

592



593

594 **Figure 3.** Examples of long-term devil and tumour dynamics. Scenario 1 is an example of
595 DFTD extirpation, and Scenario 2 is an example of coexistence. The upper panels show the
596 summarized population sizes (free-ranging individuals ≥ 35 weeks old) over 100 years (5,200
597 weeks) of simulations after the introduction of DFTD in the population, middle panels show
598 the respective wavelet power spectra, based on Morlet wavelet analysis. Red colours in the
599 power spectra show periodicity (measured in weeks) of highest intensity with ridges (black
600 lines) at frequencies often > 500 weeks. Lower panels show the prevalence of DFTD
601 (growing tumour $\geq 0.1 \text{ cm}^3$) in the respective population.

602

603

604

605

606

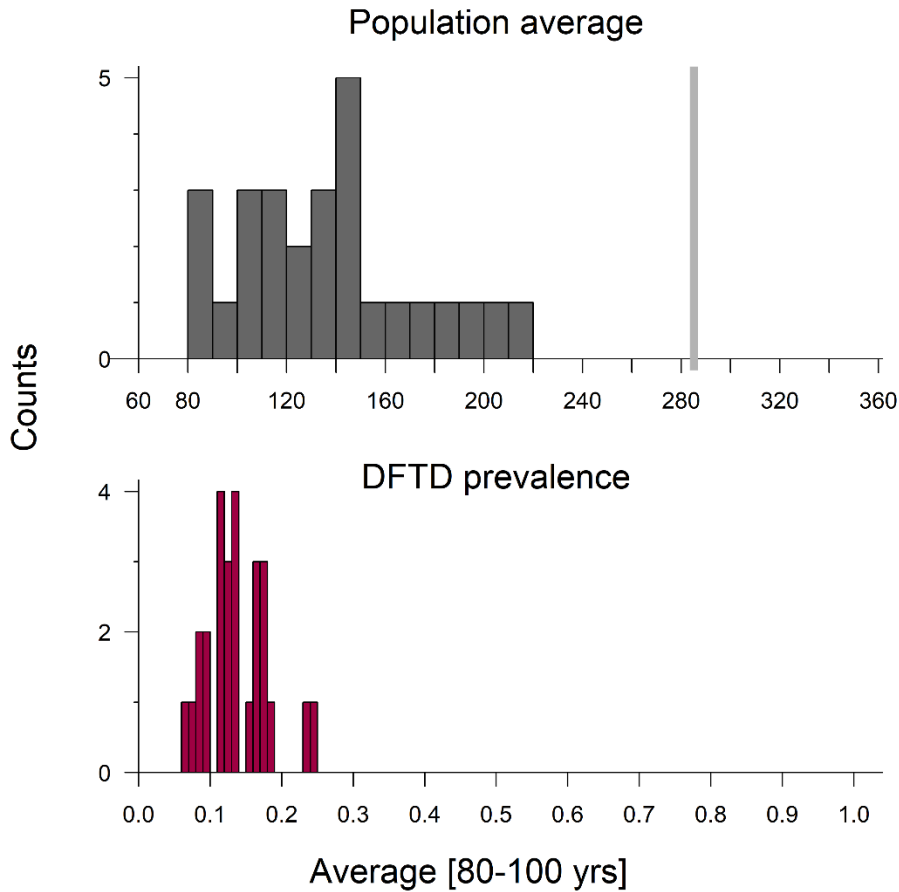
607

608

609

610

611



612

613 **Figure 4.** Frequency distributions (count) of mean devil populations sizes (x axis, upper
614 panel) and devil facial tumour disease (DFTD) prevalence (x axis, lower panel) 80-100 years
615 after disease introduction for those scenarios ($n = 27$) in which DFTD persisted for at least
616 100 years. The light-grey vertical line in the upper panel indicates the mean population sizes
617 of simulated populations over 100 years prior to disease introduction.